



# Climatic, topographic, and anthropogenic factors determine connectivity between current and future climate analogs in North America

Carlos Carroll<sup>1</sup> | Sean A. Parks<sup>2</sup> | Solomon Z. Dobrowski<sup>3</sup> | David R. Roberts<sup>4,5</sup>

<sup>1</sup>Klamath Center for Conservation Research, Orleans, California, USA

<sup>2</sup>Aldo Leopold Wilderness Research Institute, Rocky Mountain Research Station, US Forest Service, Missoula, Montana, USA

<sup>3</sup>Department of Forest Management, College of Forestry and Conservation, University of Montana, Missoula, Montana, USA

<sup>4</sup>Department of Geography, University of Calgary, Calgary, Alberta, Canada

<sup>5</sup>Arctic Institute of North America, University of Calgary, Calgary, Alberta, Canada

## Correspondence

Carlos Carroll, Klamath Center for Conservation Research, Orleans, CA 95556, USA.

Email: carlos@klamathconservation.org

## Funding information

Wilburforce Foundation

## Abstract

As climatic conditions shift in coming decades, persistence of many populations will depend on their ability to colonize habitat newly suitable for their climatic requirements. Opportunities for such range shifts may be limited unless areas that facilitate dispersal under climate change are identified and protected from land uses that impede movement. While many climate adaptation strategies focus on identifying refugia, this study is the first to characterize areas which merit protection for their role in promoting climate connectivity at a continental extent. We identified climate connectivity areas across North America by delineating paths between current climate types and their future analogs that avoided nonanalogous climates, and used centrality metrics to rank the contribution of each location to facilitating dispersal across the landscape. The distribution of connectivity areas was influenced by climatic and topographic factors at multiple spatial scales. Results were robust to uncertainty in the magnitude of future climate change arising from differing emissions scenarios and general circulation models, but sensitive to analysis extent and assumptions concerning dispersal behavior and maximum dispersal distance. Paths were funneled along north-south trending passes and valley systems and away from areas of novel and disappearing climates. Climate connectivity areas, where many potential dispersal paths overlapped, were distinct from refugia and thus poorly captured by many existing conservation strategies. Existing protected areas with high connectivity values were found in southern Mexico, the southwestern US, and western and arctic Canada and Alaska. Ecoregions within the Isthmus of Tehuantepec, Great Plains, eastern temperate forests, high Arctic, and western Canadian Cordillera hold important climate connectivity areas which merit increased conservation focus due to anthropogenic pressures or current low levels of protection. Our coarse-filter climate-type-based results complement and contextualize species-specific analyses and add a missing dimension to climate adaptation planning by identifying landscape features which promote connectivity among refugia.

## KEYWORDS

climate change adaptation, connectivity, conservation planning, graph theory, protected areas, refugia

This is an open access article under the terms of the Creative Commons Attribution License, which permits use, distribution and reproduction in any medium, provided the original work is properly cited.

© 2018 The Authors. *Global Change Biology* Published by John Wiley & Sons Ltd.

## 1 | INTRODUCTION

In coming decades, much of the earth's biota will experience climatic conditions outside the range to which they are adapted (Mora et al., 2013). Some populations will be able to persist in place in climatic refugia within their current range (Keppel & Wardell-Johnson, 2012). However, persistence of many populations will hinge on their ability to disperse and colonize habitat which has become newly suitable for their climatic requirements. Opportunities for such dispersal and range shifts may be limited unless areas that play a key role in facilitating dispersal under climate change (which we term “climate connectivity areas” after McGuire, Lawler, McRae, Nuñez, and Theobald (2016)) are identified and protected from land use that may impede movement (Heller & Zavaleta, 2009).

Identifying areas that promote climate connectivity is challenging given the diverse and multifaceted nature of biotic response to climate change, as well as uncertainty as to the pace and pattern of change arising from contrasts between projections based on different atmosphere-ocean general circulation models (AOGCM) and emission pathways. In order to allocate conservation resources to maximize the persistence of species in the face of climate change, planners need robust answers to such questions as: What areas will provide key dispersal routes as climate shifts? Do such routes overlap with areas heavily altered by humans? Where do dispersal routes for different species or routes connecting different climatic niches overlap? Are these areas associated at local, regional, and continental extents with topographic and other features that could help us predict their locations? And finally, will areas that promote connectivity in the near future remain important as climate change strengthens in the more distant future?

The concept of *centrality* provides a novel and informative approach to addressing such questions. Many habitat connectivity analyses apply models which treat landscapes as graphs, defined in this sense as a networks of nodes linked along edges (Carroll, McRae, & Brookes, 2012; Newman, 2010) (Supporting information Figure S1, Table S1). Edges, which represent functional connections (e.g., dispersal) between nodes, are assigned weights that represent an attribute such as habitat quality. A sequence of nodes connected by edges forms a path. Although abstracted depictions of landscape pattern, graphs may reveal emergent aspects of landscape structure that are not otherwise discernible.

Most graph-based analyses focus on delineating paths between individual source and target patches (Adriaensen et al., 2003). Betweenness centrality (henceforth centrality) metrics instead evaluate paths between all or a subset of pairwise combinations of sites on a landscape to rank the contribution of each site to facilitating dispersal across the network of sites (Ahuja, Magnanti, & Orlin, 1993; Newman, 2010). Areas of high centrality emerge as conservation priorities because the loss of sites where many paths overlap would disproportionately lengthen dispersal distances or transit times between nodes and thus disproportionately reduce dispersal across the network (Álvarez-Romero et al., 2018; Carroll et al., 2012).

This paper develops a novel approach that extends previous work in several ways (Table S2). Initial efforts to identify climate connectivity areas made the simplifying assumption that such areas can be identified based solely on current climate or other environmental characteristics. For example, Nunez et al. (2013) identified climate connectivity areas by connecting patches of intact habitat with other patches that had a cooler climate under current conditions, in order to provide migration routes as climate warmed. In contrast, subsequent work by McGuire et al. (2016) connected source patches to destination patches projected to be similar or cooler under future climates. Littlefield, McRae, Michalak, Lawler, and Carroll (2017) extended this approach by evaluating dispersal potential between climatically analogous current and future patches via paths that avoided human-modified habitat.

Climatic velocity is a metric often used to assess geographic patterns of climate exposure (Loarie et al., 2009). Climatic velocity values are often based on the straight-line distance between a climate type and the nearest location of the analogous climate type under future climates (Hamann, Roberts, Barber, Carroll, & Nielsen, 2015; Ordóñez & Williams, 2013). Because the assumption of straight-line dispersal is often unrealistic for terrestrial flora and fauna, Dobrowski and Parks (2016) developed a velocity metric based on the shortest or least-cost path between current and future climate analogs that avoided nonanalogous climates, which is typically longer than a straight-line path. The rationale for this approach is similar to that underlying climatic niche models: if climate is a key habitat factor for an organism, climatically hostile areas that deter movement to newly suitable habitat will threaten persistence under climate change.

In this study, we developed a centrality metric which combines the climatic-resistance-based approach of Dobrowski and Parks (2016) with methods of evaluating dispersal potential similar to those of Littlefield et al. (2017). We identified priority areas for connectivity under climate change by connecting current and future climate analogs along paths that minimize exposure to nonanalogous climates (Dobrowski & Parks, 2016). Centrality based on climatic resistance has previously been used to identify key dispersal areas for marine systems (García Molinos et al., 2017). This study represents the first application of climatic-resistance-based centrality to terrestrial systems under climate change. We synthesized results from all climates occurring in North America to identify areas of high centrality whose loss could potentially impact many organisms, and to discern what aspects of continental and regional topography help explain broad-scale connectivity patterns. We evaluated connectivity across the landscape as a whole rather than solely between patches with low degree of human modification. We compared priorities identified by two methods (shortest- and current-flow-based paths) that make contrasting assumptions about the ability of dispersers to find and follow optimal paths (Carroll et al., 2012). We compared connectivity areas important in the near future to those important in the more distant future to assess whether priorities are robust to time horizon. Finally, we assessed the vulnerability of key climate connectivity areas by

evaluating the extent to which they fall within existing protected areas, or conversely within areas where high human land use intensity might impede movement. Our approach, which can be applied at a range of scales, avoids many of the simplifying assumptions of previous studies, allowing planners to more realistically assess where conservation resources should be directed to protect climate connectivity areas and facilitate persistence of species under climate change.

## 2 | MATERIALS AND METHODS

### 2.1 | Climate data

Climate data used here cover the North American continent (excluding areas south of Mexico), a study area which includes a diverse set of ecoregions that vary widely in their topographic, climatic, and biotic attributes. To represent current climate, we used modeled estimates of 1981–2010 monthly temperature and precipitation (Lambert Azimuthal Equal Area projection) as derived by the ClimateNA software (Wang, Hamann, Spittlehouse, & Carroll, 2016). ClimateNA data at 1 km resolution were resampled to 5 km resolution to increase computational feasibility as described below. ClimateNA current climate data are in turn based on data developed by the PRISM project, which used regression to interpolate weather station data based on location, elevation, coastal proximity, topographic facet orientation, vertical atmospheric layer, topographic position, and orographic effectiveness of the terrain (Daly et al., 2008).

Projections of future climate (as monthly mean temperature and precipitation) were derived from the Coupled Model Intercomparison Project phase 5 (CMIP5) database which includes AOGCMs corresponding to the 5th IPCC Assessment Report (Wang et al., 2016). For the main analysis, future projected temperature and precipitation were calculated as anomalies from the current (1981–2010) reference period to the future 2071–2100 period (hereafter “2080s”), based on an ensemble mean of 15 representative CMIP5 AOGCMs for representative concentration pathway (RCP) 8.5, a “business-as-usual” scenario characterized by relatively high greenhouse-gas emissions (Wang et al., 2016). We also compared results from the main analysis with results from additional future time periods and RCPs as part of the sensitivity analysis described below. Anomaly grids were downscaled via local regression and the difference was added to the baseline climate normal data to arrive at the final climate surface (Wang et al., 2016).

From the monthly temperature and precipitation gridded datasets, we developed 11 bioclimatic variables (Table S3) that were more directly related to ecological factors (Wang et al., 2016). We used principal components analysis (PCA) to reduce the dimensionality of the 11 climate variables, which reduced collinearity and increase computational feasibility in subsequent stages of the analysis. Following Carroll et al. (2017), we used climate data based on the PCA's first 2 axes (hereafter PC1 and PC2), which explained 89.3% of variance (Table S3).

### 2.2 | Centrality metrics

We adapted the methods of Dobrowski and Parks (2016) to delineate paths between current and future climate analogs that jointly minimized geographic distance and exposure to increasingly dissimilar climate based on a cost penalty parameter. However, we used multivariate climate surfaces rather than mean annual temperature as did Dobrowski and Parks (2016). We defined 100 equal-width climate types for each of the first two PCA axes. Approximately one third of the 10,000 potential unique combinations of PC1 and PC2 occur under current North American climates. Previous sensitivity analyses (Carroll, Lawler, Roberts, & Hamann, 2015; Hamann et al., 2015) suggested that classifications resulting in several thousand types represent a good balance between the extremes of loss of information due to excessively broad types vs. domination of the results by disappearing or no-analog climates due to excessively narrow types. An approach based on equal-width climate types does not incorporate information on the historical range of local climatic variability at a site (Mahony, Cannon, Wang, & Aitken, 2017); incorporating such information would represent a useful future extension of our method.

For all pixels of each current climate type (i.e., unique combination of PC1 and PC2) in North America, we identified all pixels with the same climate type in the future time period. A pixel is used here to represent a unit of geographic space, as distinguished from a climate type, which represents a subdivision of climatic space (Table S1). We developed cost surfaces (one for each climate type) in a manner that accounts for spatiotemporal changes in climate, allowing isoclines to be traced over landscapes and through time. To do so, we first interpolated current and future PC1 and PC2 grids to represent incremental changes over the current to future time period (Supporting information Figure S2). These interpolated grids represent incremental changes in multivariate climate conditions between current (1981–2010) and future period (2071–2100) and assume a linear trend in changes in climate over this time period.

We created cost surfaces (Supporting information Figure S2) for each of these interpolated climate grids such that costs were proportional to the level of dissimilarity between PCA values of the pixel of interest under current climate and all other pixels. We adapted the methods of Dobrowski and Parks (2016) to our multivariate approach by adding the dissimilarity values from the two PCA axes and multiplying by a cost penalty value of two dimensionless units such that cost increased by two for each increase in dissimilarity of one scaled PCA units (see Supporting information Text S1 for code). Lakes and ocean were arbitrarily assigned a cost value of 5,000 to force trajectories to avoid water when possible. We then calculated, among all intermediate cost surfaces, the minimum cost for each pixel; this minimum cost is used to generate the final cost surface for each climate type.

By basing resistance on the minimum cost for the entire period, we sought a computationally efficient approximation that would allow trajectories between source and destination locations to follow the climate as it changes and avoid traversing dissimilar climates. For example, assuming a source pixel in the southern Great Plains region and a destination pixel in the northern Great Plains region with little

intervening topographic variation, an organism following the minimum cost surface could shift at the same rate as climate changed without experiencing dissimilar climates.

Although the minimum-resistance approach provides a good approximation in flatter terrain, it is less accurate in topographically complex terrain where there may be a temporal mismatch between the timing of potential range expansion through a given pixel and the resistance value assigned to that pixel. For example, an area of similar climate (and hence low resistance) might be present in a distant valley in the near future, but minimum resistance would not accurately reflect the climate experienced by an organism when that area was transited in the distant future, and might identify overly simplified (i.e., straighter) paths.

An alternative approach explicitly considers the temporal ordering of climate-based resistance in a step-wise fashion, by identifying paths for each intermediate timestep and linking these paths into continuous chains across the entire time period of interest using network flow algorithms (Alagador, Cerdeira, Araújo, & Saura, 2014; Graham, Vanderwal, Phillips, Moritz, & Williams, 2010; Phillips, Williams, Midgley, & Archer, 2008). However, such algorithms are currently too computationally intensive for analysis at the extent and resolution considered here (Alagador, Cerdeira, & Araújo, 2016; Carroll et al., 2012). In addition, our approach implicitly assumes that organisms are adapted to the current climate at a location, and any departure from the current climate type should be avoided. We do not consider factors such as competition or the relationship of local climate to the species climatic niche as a whole, which could result in an organism experiencing increased fitness under altered climate.

For each climate type, a raster of centrality values was calculated using the set of source and target pixels for each climate type identified previously. Values derived from this type of input are termed subset centrality because source and target nodes are a subset of the network as a whole, although in total across all subsets (climate types) they encompass the entire network (Carroll et al., 2012). We summed centrality results across all climate types in order to give equal weight to all pixels. An alternate approach which weighted common and rare climate types equally irrespective of their geographic extent gave similar results (Spearman's rank correlation ( $\rho$ ) of centrality values = 0.93).

We evaluated centrality using two contrasting types of graph-based algorithms (shortest-path and current flow; Newman, 2010). The primary approach used current-flow algorithms based on electrical circuit theory that treat landscapes as conductive surfaces, that is, networks of nodes connected by resistors. These models are widely applied in ecological research and conservation planning, and model predictions have been shown to correlate with dispersal routes and gene flow (McRae & Beier, 2007). When current is injected into a source node and allowed to flow across a network until it reaches a target node, the amount of current flowing through each intermediate node reflects the likelihood that a random walker leaving the source node, and moving along edges with probabilities inversely proportional to their resistance weights, will pass through the intermediate node on its way to the target node.

Current-flow-based methods assume that dispersers have limited knowledge about distant habitats, and thus a high degree of

randomness in their dispersal routes (McRae & Beier, 2007). The models integrate the contributions of all possible pathways across a landscape or network, rather than a single shortest path (Supporting information Figure S1). As in electrical circuits, the addition of new pathways increases total connectivity but may reduce the flow on any particular path by distributing flow across more routes (McRae & Beier, 2007). Areas of high current-flow centrality correspond to areas of constrained connectivity where few alternate routes exist (McRae et al., 2016). Areas of low centrality may either experience no dispersal flow or diffuse dispersal along many alternate routes.

We calculated current-flow centrality using the *passage* function of the *gdistance* package in R (van Etten & Hijmans, 2010), with the theta parameter set to 0, the default corresponding to current flow. Although van Etten and Hijmans (2010) refer to the resulting values as "passage density," they are equivalent to the more widely used term "centrality." Calculation of centrality, especially current-flow centrality, is computationally intensive, as the complexity of the problem increases quickly with an increase in the number of nodes or pixels considered. Given  $n$  source pixels and  $m$  target pixels, complexity is on the order  $n^2(n + m)$  for current-flow methods, vs.  $nm + n^2/\log(n)$  for the shortest-path methods described below (Ahuja et al., 1993). A single current-flow centrality raster was calculated for each climate type using all current locations of that type as sources and all future locations of that type as targets (Figure 1). Calculation at the extent of North America at 5 km resolution required approximately one week on a 16-core server with 256 GB RAM.

We characterized the results of the current-flow centrality analysis in terms of their distribution in climatic space. We first plotted in climate space (i.e., in terms of PCA1 and PCA2 axes) the sum of the centrality values (for all climate type rasters) found in the spatial locations characterized by each climate type. Each pixel in climate space in these plots represents the connectivity value of the geographic areas which exhibit this climate type. We then plotted the maximum values from the entire raster (i.e., for all geographic areas) of centrality results for each climate type onto a plot of the two PCA axes, both as an unscaled value and as a value divided by the total centrality values for that climate type raster. Each pixel in climate space in these latter plots represents the maximum value across all North America of the centrality map connecting current and future analogs of a single climate type. Climate types with high maximum centrality may have constrained connectivity with their future analogs (i.e., dispersal is limited to a few alternative routes).

### 2.3 | Sensitivity of current-flow results to alternative model structures and extents

We analyzed three alternative current-flow-based models or scenarios to discern the effects of different aspects of the model in producing observed centrality patterns. Firstly, what we term the "full model," which connects present-day climate types to future analogs across a climate-type-specific resistance layer as described above, was used to identify areas of high centrality resulting from constraints imposed by climatic gradients in the intervening landscape. Secondly, the "uniform-resistance model," which connects present-

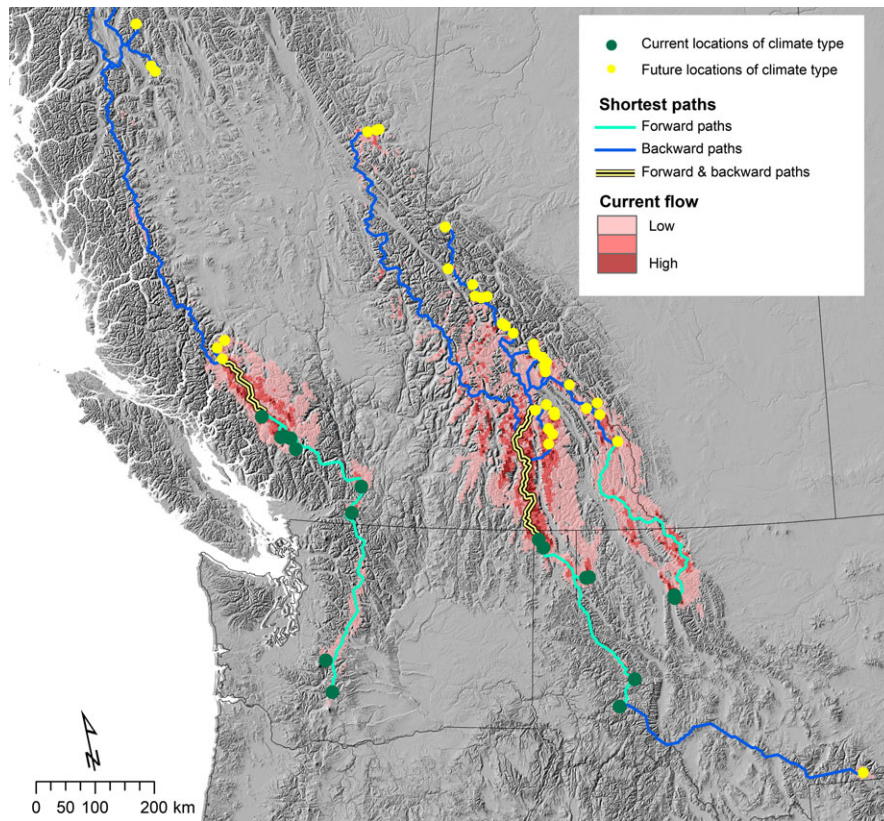


**FIGURE 1** Map of shortest-path and current-flow analysis results for an example climate type located in western North America. Forward shortest paths connecting each current climate location to its closest future analog differ from backward shortest paths connecting each future climate location to its closest current analog. Current-flow centrality results connect all current and future locations of the climate type by means of diffuse flow rather than single paths

day climate types to future analogs across a uniform resistance layer, was used to identify areas of high centrality resulting from the geographic distribution of climate types without consideration of the intervening landscape. The contrast between the uniform resistance and full model is analogous to the contrast between Euclidean (straight-line) distance-based climatic velocity metrics and the minimum-exposure-distance-based velocity metric of Dobrowski and Parks (2016). Finally, the “null model” which connects all points across a uniform resistance layer, was used to identify areas of high centrality resulting from the shape of the North American continent.

We assessed sensitivity of results to the spatial extent of analysis by comparing results from the continental-extent current-flow analysis with those from an analysis at the extent of an example ecoregion, at both 1 and 5 km resolutions. We selected for this comparison an ecoregion (the Central Basin and Range ecoregion of the interior western US; C.E.C., 1997) which encompasses a large temperature and precipitation gradient. We buffered the ecoregion by 200 km to reduce edge effects.

## 2.4 | Sensitivity of results to alternative GCMs and RCPs

To evaluate sensitivity to parameter uncertainty, we also ran the full model using eight representative CMIP5 AOGCMs (CCSM4, CNRM-

CM5, CanESM2, GFDL-CM3, HadGEM2-ES, INM-CM4, IPSL-CM5A-MR, and MPI-ESM-LR; Knutti, Masson and Gettelman, 2013) for both RCP8.5 and a more moderate emissions pathway (RCP4.5) for the 2080s periods. We also ran the full model based on AOGCM ensemble predictions for current to near-future (2050s) projections, and near-future to distant-future (2080s) projections. We compared resultant centrality values using Spearman rank cross-correlation coefficients which provide the mean correlation (i.e., across the entire geographic space) between two rasters expressed as matrices. Parameter sensitivity analyses were performed at 10 km resolution to increase computational feasibility, a decision supported by our finding that results from the full model at 5 km were highly correlated with those obtained at 10 km ( $\rho = 0.96$ ).

## 2.5 | Comparison of current-flow centrality results with other climatic and nonclimatic variables

We hypothesized that current-flow centrality results would not be strongly correlated with climatic and topographic variables previously used to identify refugia, but that nonlinear relationships might exist that would be informative in interpreting centrality patterns at the continental extent. We compared centrality output from the full model to seven additional variables using: cross-correlation coefficients and generalized additive models (GAM; Hastie & Tibshirani,

1990). The seven variables included four nonclimatic variables (latitude, elevation, elevational diversity, and topographic position index). Elevation data for North America were resampled to 1 km resolution from an original resolution of 1 arc-second (~30 m) (ASTER; ASTER GDEM Validation Team, 2009) to 3 arc-second (~90 m) (SRTM; Farr et al., 2007). We then derived elevational diversity values as in Carroll et al. (2017), using a form of Rao's quadratic entropy (Rao, 1982), by measuring the mean elevation contrast between all pairs of pixels within a spatial neighborhood defined by the moving window of the specified extent (here 27 by 27 km after Carroll et al. (2017)). Topographic position index (TPI) measures the elevational position of a 5 km pixel in relation to its surrounding neighborhood (here 81 by 81 pixels after Stralberg et al. (2018)) as the pixel elevation divided by the mean elevation of the surrounding neighborhood (Wilson, OConnell, Brown, Guinan, & Grehan, 2007).

The seven variables also included three climatic variables (climatic dissimilarity, forward climatic velocity, and backward climatic velocity). We defined climatic dissimilarity as the Euclidean distance in PCA climatic space between current and future climate at a pixel. Forward and backward climatic velocities were defined using the analog-based method and represent the straight-line distance between analogs (Hamann et al., 2015). To evaluate the relationship between connectivity areas and refugia, we also categorized EPA Level III ecoregions ( $n = 182$ ) into four quadrants based on high and low centrality and backward climatic velocity values.

## 2.6 | Comparison of current-flow and shortest-path centrality

We compared results from the full current-flow-based model with shortest-path centrality values derived using methods adapted from Dobrowski and Parks (2016). Shortest-path models represent cost (e.g., energetic cost or mortality risk) of movement through different habitat (here climate) types as distance (i.e., points in less permeable habitat are conceived as farther apart), in order to identify the route between two predetermined endpoints that has the shortest total distance (least total cost) in terms of the summed resistance of all pixels on the path (Newman, 2010). Shortest-path methods effectively assume that dispersers have complete knowledge about values of distant habitats.

Although the dispersal model underlying shortest-path metrics may be less realistic than that underlying current-flow metrics, the greater computational feasibility of shortest-path algorithms allowed us to calculate paths on a pairwise basis between each source location of a climate type in time period A and the target location in the time period B which was "closest" in terms of summed resistance (Figure 1). This allowed us to assess the sensitivity of centrality values to assumptions regarding maximum dispersal distance thresholds, by comparing results from all path lengths with results which excluded paths of greater than a threshold value (termed bounded-distance centrality; Newman, 2010). We also compared shortest-path centrality results with current-flow centrality and the seven environmental variables described above.

We calculated shortest paths in both forward and backward directions (Figure 1), which are analogous to the forward and backward versions of climatic velocity (Hamann et al., 2015). Backward climatic velocity represents the distance and rate at which organisms adapted to a location's future climate will need to move to reach that location, and reflects a location's ability to serve as a refugium (Carroll et al., 2015). In contrast, forward climatic velocity, which represents the rate at which an organism currently at a location must move to find future suitable climate, is more relevant to measuring threats to organisms themselves. Forward velocity will often be high in alpine areas because reaching the nearest analogous future climate may require dispersal to distant higher elevation mountaintops (Carroll et al., 2015). Conversely, backward velocity is generally low in alpine areas, because adapted organisms can reach the site from nearby downslope locations. Values are often high in valley bottom habitat because organisms must travel longer distances to colonize these locally new habitat conditions. Because pairwise paths between all current and future locations of a climate type are analyzed jointly during the current-flow calculations, the distinction between the forward and backward directions is not relevant to current-flow centrality results (Figure 1). Therefore, we aggregated forward- and backward shortest path output when comparing shortest-path centrality to current-flow centrality.

## 2.7 | Protected areas and land use

For these two analyses, we reclassified centrality values into quantiles within each EPA Level I ecoregion (which categorize North America into 15 large regions) to ensure priorities were identified in all broad biome types despite the strong latitudinal gradient in centrality. We evaluated the performance of the current system of protected areas in North America (IUCN categories I (strict nature reserve)—VI (sustainable use area); C.E.C., 2010) in capturing climate connectivity areas by measuring the mean centrality value within and outside of the current protected area system. We overlaid maps of centrality on data depicting anthropogenic land use intensity, and ranked EPA Level III ecoregions in terms of both metrics. We used the most recent (2009) values for the Human Footprint, which combines values from eight input layers to create a composite human influence index ranging from 0 (no human influence) to 50 (maximum human influence possible under the methods of Venter et al. (2016)).

# 3 | RESULTS

## 3.1 | Distribution of high centrality areas in climatic space

Mean annual temperature and precipitation were the variables with the highest loadings on our PCA axes 1 and 2, respectively (Supporting information Table S3, Figure S3). However, several other bioclimatic variables had similarly high contributions, resulting in PCA axes that incorporated more information than would have occurred if only mean annual temperature and precipitation had been used. Areas

which had high centrality (as summed over all climate types) were primarily located in the wettest and coldest portions of climate space under both current and future climates (Supporting information Figure S4a,b). The climate types which were most constrained in terms of connectivity between current and future climates (as measured by their maximum centrality values) were more broadly distributed in climate space, and were more common in hot semi-arid climate types than in wetter regions (Supporting information Figure S4c,d).

### 3.2 | Comparison of centrality with other landscape metrics

Current-flow centrality values were only weakly correlated (Spearman's rank correlation ( $\rho$ ) < 0.30) with six of the seven variables considered (elevation (0.17), elevational diversity (0.21), topographic position index (0.04), climatic dissimilarity (0.29), forward climatic velocity (0.22), and backward climatic velocity (-0.06)). Greater rank correlation was shown between current-flow centrality and latitude (0.46). A four-quadrant categorization of North American EPA Level III ecoregions ( $n = 182$ ) in terms of their backward climatic velocity (which is inversely related to potential value as climate refugia) and current-flow centrality (Figure 2) showed much of the high Arctic to have both high climatic velocity and high centrality (Supporting information Figure S5). Ecoregions with low velocity and high centrality were located in areas such as the Isthmus of Tehuantepec in southern Mexico, due to their combination of a large elevational gradient, which created local refugia, in addition to a geographic location which facilitated broad-scale climate connectivity. Shortest-path centrality values were not strongly correlated ( $\rho < 0.16$ ) with any of the seven variables considered (latitude (0.02), elevation (0.15), elevational diversity (0.04), topographic position index (0.05), climatic dissimilarity (0.003), forward climatic velocity (0.004), and backward climatic velocity (-0.15)).

The results of the generalized additive models (GAM) with single predictors demonstrated that relationships between current-flow centrality and topographic variables are nonlinear (Supporting information Figure S6, Table S4). All climatic metrics showed an increasing trend with latitude. Climate dissimilarity and forward velocity showed a stronger trend than did centrality and backward climatic velocity (Supporting information Figure S6a), due to polar amplification of the pace of climate change (Huang et al., 2017) in the case of climate dissimilarity, and to the northern continental edge leading to disappearing climate types in the case of forward velocity. In interpreting the GAM results, note that planners would typically seek to conserve areas with high values for centrality (i.e., potential connectivity areas) but low values for climatic dissimilarity and velocity (i.e., potential refugia).

We found a quadratic relationship between current-flow centrality and topographic position index (TPI) which demonstrated an association between centrality and both ridgelines and valley bottoms, with lowest values in flat areas (Supporting information Figure S6c). A multivariate GAM containing latitude, TPI, and their interaction term suggested that valley bottoms were important for

connectivity at all latitudes, but ridgelines were most important at high latitudes (Supporting information Figure S6d).

The geographic distribution of current-flow centrality values was consistent with GAM results, in that high values were found along major north-south-oriented passes (Figure 2b). Long north-south oriented mountain chains also showed high importance, although centrality was often greatest in midslope areas rather than along summits (Figure 2d). Paths tend to avoid areas of high forward velocity and disappearing climates, especially in lower latitudes, with centrality increasing in the interstices between such areas as paths were constrained to a few potential routes (Figure 2c).

### 3.3 | Robustness of priorities to AOGCM, RCP, time period, and extent

Results of the sensitivity analysis suggested that current-flow centrality values were highly robust to parameter or data uncertainty caused by variation between AOGCM projections, emission pathways, and time horizon. Rank correlation between results from the eight AOGCMs was 0.92 for RCP4.5 and 0.93 for RCP8.5. Rank correlation between results from RCP4.5 and RCP8.5 projections was 0.96. The high rank correlation (0.92–0.96) between results from different time periods demonstrated a high degree of similarity between near-future and distant-future climate connectivity areas.

However, current-flow centrality results for our example ecoregion (Central Basin and Range) were sensitive to analysis extent. Only moderate rank correlation (0.66) was shown between results at 5 km resolution from the continental- and ecoregional-extent analyses, although general patterns were similar (Figure 3). Ecoregional-extent analyses were highly correlated at resolutions of 5 km vs. 1 km (0.95).

### 3.4 | Contrasts between alternative current-flow models

Results from the null model (Supporting information Figure S7a), which connected all points across a uniform resistance layer, showed areas of high centrality resulting from the shape of the North American continent. Limited path options and hence high centrality values were generated along coastal isthmuses (e.g., the Isthmus of Tehuantepec) and peninsulas (e.g., Aleutian), and between large lakes, as well between Hudson Bay and the Arctic Ocean.

Results from the uniform-resistance model (Supporting information Figure S7b), which connected current climate types to analogous future types across a uniform resistance layer, showed areas of high centrality resulting from the geographic distribution of current climate types relative to their future analogs, but without consideration of climatic heterogeneity of the intervening landscape. In addition to the areas evident in the null model, high centrality was shown more widely across western Canada and southern Alaska, especially along the Pacific coastal ranges. Additional areas were evident in the interior of the continent, especially the western US.

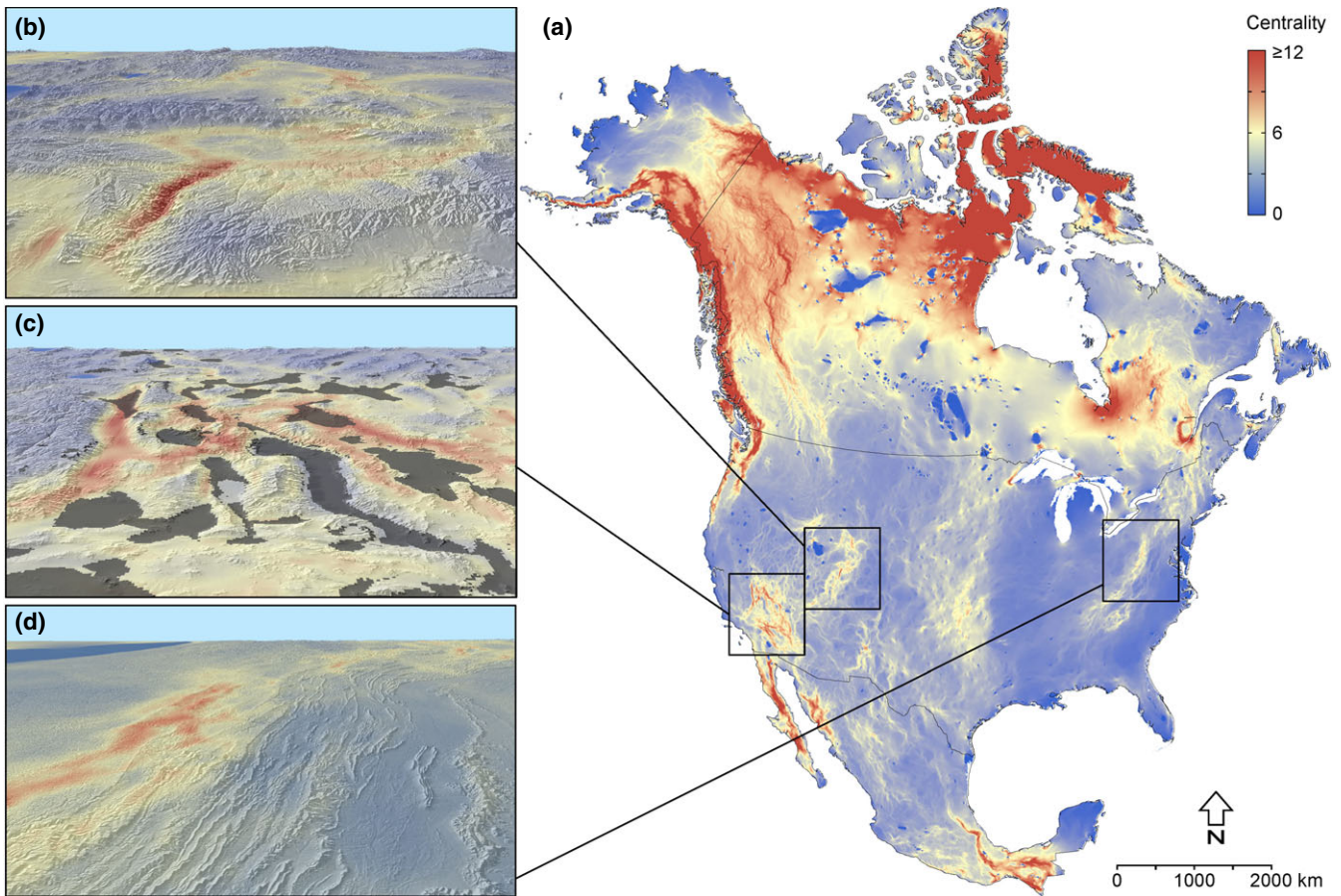


**FIGURE 2** Results of the current-flow centrality analysis of connectivity in North America between current (1981–2010) and projected future (2071–2100) climate types. Current-flow centrality values (a) represent the net flow of dispersers through a site, and assumes a degree of randomness in dispersal movements. High values were found within north-south trending passes (b) and ridge systems (d), and may avoid areas with disappearing or novel climate types (gray areas in (c))

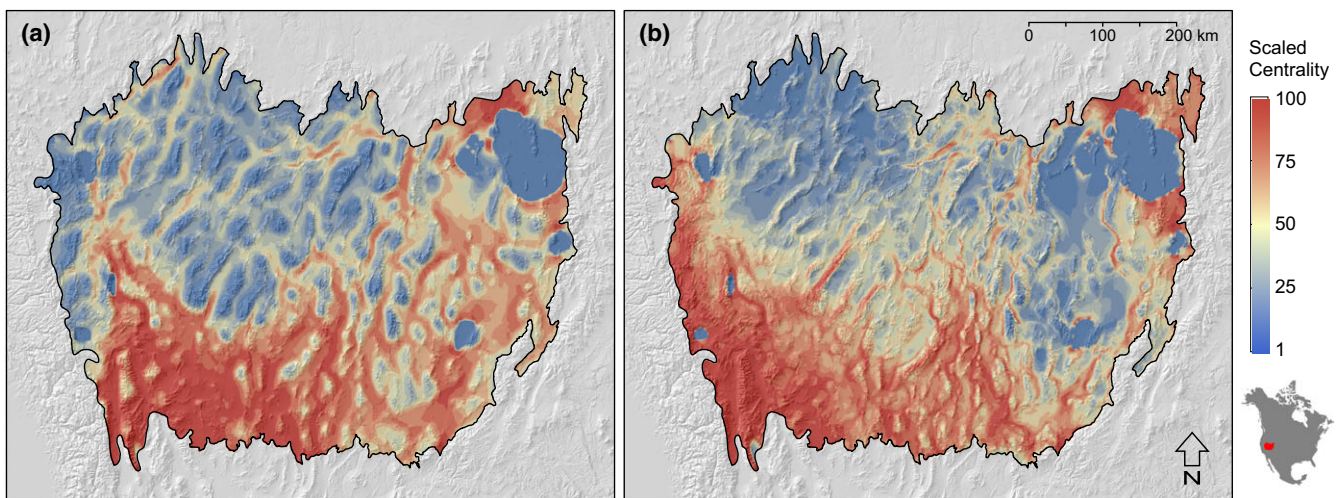


**FIGURE 3** Contrasts between results of current-flow centrality analysis at two spatial extents, depicting connectivity between current (1981–2010) and projected future (2071–2100) climate types, for the Central Basin and Range ecoregion of the interior western US: (a) as subset from results of the continental-extent analysis (Figure 2), and (b) for an analysis extent limited to the ecoregion and a 200 km buffer region to reduce edge effects. The two rasters were rescaled to 100 equal-area quantiles for comparability

Results from the full model (Figure 2), which connected current climate types to analogous future types across a type-specific climatic resistance layer, showed areas of high centrality resulting from constraints imposed by climatic gradients in the intervening landscape. Fine-resolution variation in centrality was added to the patterns evident in the null and uniform-resistance models, especially in topographically complex regions of western North America.

Rank correlation between results of the uniform-resistance model and full model was 0.84. Partial rank correlation between full and uniform-resistance after accounting for the common influence of continental shape (null model) was 0.82, indicating that most commonality between results was attributable to the distribution of climate types, and little to continental shape.

### 3.5 | Shortest-path centrality

Shortest paths were on average 1.45 times the length of straight line distances between climate analogs (Supporting information Figure S8). Paths tended to be located along north-south trending mountain ranges, but fell on the drier or leeward slopes rather than along summits (Figure 4). Straight paths across the interior plains represent artifacts of this method, which will always identify an optimal path, which may be a straight line across relatively featureless landscapes. Forward (current-to-future) shortest-path results were not strongly correlated with backward shortest-path results ( $\rho = 0.29$ ). Whereas forward shortest-path centrality was highest along interior cordilleras such as the Rocky and Appalachian ranges (Figure 4a), areas of high backward shortest-path centrality were more widely distributed and included coastal ranges (Figure 4b). GAM relationships between shortest-path centrality and topographic variables were weaker than those shown by current-flow centrality (Supporting information Figure S6, Table S4), but indicated that backward shortest-paths tended to fall at lower elevations and along valleys rather than ridges (Supporting information Figure S6b,c).

The minimum path length within a 5 km pixel was relatively low for both forward and backward centrality within montane regions outside of high latitude regions, and relatively high in nonmontane and high-latitude regions (Supporting information Figure S9). Target pixels (destinations of dispersers) for forward shortest-paths were concentrated in coastal and interior montane regions and the high Arctic, whereas target pixels (origins of dispersers) for backward shortest-paths were more widely distributed (Supporting information Figure S10).

Comparison of the mean values by EPA Level III ecoregion between current-flow and shortest-path centrality analyses (Figures 2 and 4) suggested that there was moderate rank correlation ( $\rho = 0.52$ ,  $n = 182$ ) between the rank of ecoregions in terms of the two metrics.

### 3.6 | Centrality, protected areas, and the human footprint

Although mean current-flow centrality values were slightly higher within protected areas than outside of such areas (6.18 vs. 5.17,

respectively), protected areas, which covered 11.4% of the continent, held only 13.3% of total current-flow centrality value. Shortest-path centrality values were similar within and outside of protected areas (path count per cell of 519 vs. 521). Human footprint values were generally lower in areas of high current-flow centrality, but not for shortest-path centrality. Rank correlation of centrality raster data with human footprint values was  $-0.48$  and  $-0.06$  for current-flow and shortest-path results, respectively.

When we reclassified current-flow centrality values into equal-area percentiles within each EPA Level I ecoregion to ensure priorities were identified in all broad biome types, the protected areas with highest values were found in southern Mexico, the southwestern US, and western and arctic Canada and Alaska (Figure 5). 22 of 182 ecoregions ranked in the top quintile of reclassified centrality values and had less than 10% of their area protected (Figure 5). Ecoregions within the Great Plains, Appalachian Mountains, Isthmus of Tehuantepec (Mexico), the high Arctic, and the Cordillera of western Canada were among those identified, with the latter three regions also being highlighted when nonreclassified centrality was considered.

When areas of high human impact were compared against reclassified current-flow centrality values, eight ecoregions (including five of the 22 identified above), located in the Isthmus of Tehuantepec or the eastern temperate forests along the US/Canada border, fell in the top quintiles of both human impact index and reclassified centrality (Figure 5). Areas of high human impact index and reclassified centrality were evident on the eastern slopes of the Appalachian Mountains (US), St. Lawrence river valley (Canada), central Plains (US), southern Mexico, northern Washington (US), southwestern British Columbia, and southeastern California (Supporting information Figure S11).

## 4 | DISCUSSION

The persistence of many species under climate change will hinge on their ability to disperse and colonize habitat which has become newly suitable for their climatic requirements. Many conservation plans focus on promoting climate adaptation by identifying climatic refugia (Keppel & Wardell-Johnson, 2012), but few have considered which areas merit protection for their role in facilitating dispersal under climate change (Littlefield et al. (2017), McGuire et al., 2016). This study, the first to characterize the location of climate connectivity areas at a continental extent, can help planners identify and protect such areas from land use that may impede movement (Heller & Zavaleta, 2009).

Our results demonstrate that the priority areas for conservation of climatic connectivity are distinct from refugia, and thus poorly captured by many existing conservation strategies. Many climate connectivity areas lie outside of protected areas and face pressure from anthropogenic land use and habitat conversion. Our results suggest that connectivity priorities are robust to uncertainty as to the magnitude of future climate change arising from differing emissions pathways and general circulation models, but vary with analysis extent and differing assumptions concerning dispersal behavior and distance.

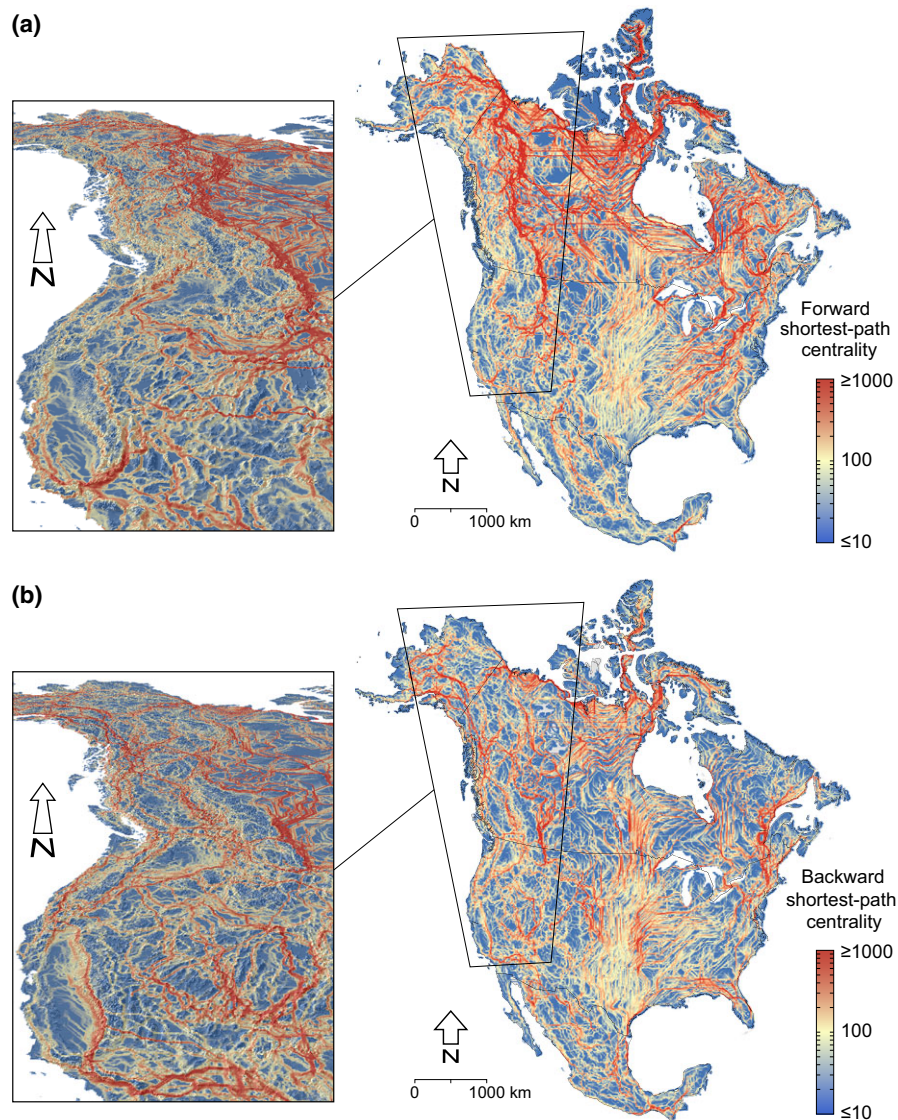


**FIGURE 4** Results of the shortest-path centrality analysis of connectivity in North America between current (1981–2010) and projected future (2071–2100) climate types. Shortest-path centrality values represent the number of overlapping dispersal paths at a site, and assume that dispersers have complete knowledge of the landscape which allows them to identify the single path with least total cost in terms of exposure to nonanalogous climate types. Forward (current-to-future) shortest paths are shown in (a), and backward (future-to-current) paths in (b)

#### 4.1 | Connectivity areas differ from refugia

Climate connectivity areas (areas which showed high current-flow centrality because large numbers of dispersal paths overlapped) did not coincide with areas of low climatic velocity (i.e., potential refugia; Keppel & Wardell-Johnson, 2012; Carroll et al. 2017), supporting the relevance of grouping sites into categories of conservation targets based on high and low centrality and refugia values (Supporting information Figure S5). The underlying cause of this contrast is that, as terrestrial organisms disperse in response to shifting climates, they must often traverse intervening nonrefugial areas to reach their targets, and are constrained by broad-scale topographic features that do not affect velocity metrics based on straight-line distances. While

velocity metrics are useful in capturing factors determining macrorefugia location, centrality captures the broad-scale factors that determine how such macrorefugia are connected by dispersal. Like velocity, centrality integrates factors operating at a range of spatial scales (Carroll et al., 2017). For example, topographically diverse areas may facilitate climate connectivity over short distances, but broad-scale topographic features such as mountain passes may be key areas for facilitating longer distance dispersal.

Both the generalized additive model (GAM) results and mapped output suggested that high centrality areas were associated with north-south trending passes and valley systems, as well as north-south trending ridgelines at higher latitudes. This latitudinal factor may be due to the fact that, in a warming climate, tropical montane

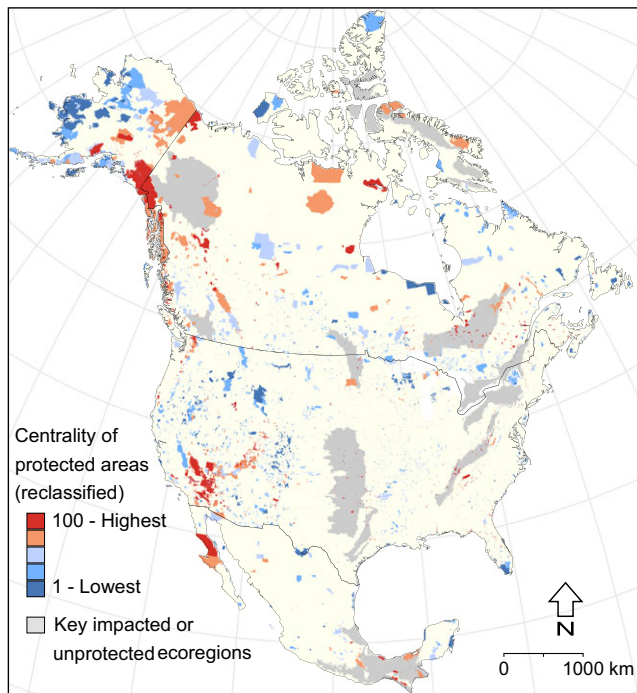


**FIGURE 5** Relative importance of major North American protected areas for climate connectivity, as measured by current-flow centrality values which had been reclassified within 15 EPA Level I ecoregions to ensure representation across broad biome types. 25 of 182 EPA level III ecoregions (areas in gray in figure) fell in the top quintile of reclassified centrality values and either had <10% of their area protected or high levels of anthropogenic pressures which placed them in the top quintile of human footprint values

areas may eventually become climatic cul-de-sacs which lack connectivity to similar climates to the north. The relationship of climatic variables to elevation suggested that protecting areas of high centrality would imply a conservation focus on different elevational zones than would a focus on protecting refugia. While ridgelines might also be identified as refugia based on their low backward climatic velocity (Carroll et al., 2017), valley bottoms would tend to be missed by refugia-based prioritizations. Areas of high forward climatic velocity and disappearing climates, especially in lower latitudes such as the desert regions of the southwestern US, tended to create bottlenecks that constrained climate connectivity (Figure 2, Supporting information Figure S4). Current-flow centrality values were also high in areas of the far north where polar amplification of climate change increased the distance between a current climate and its future analogs (Huang et al. 2017), and the shape of the continent funneled dispersal paths into limited areas.

The current protected area system does not capture climatic connectivity areas much above what would be expected by random placement. However, existing protected areas in the southwestern US and north Pacific coast of British Columbia and Alaska include areas of high centrality. Expansion of the human footprint associated with exurban growth in these regions (e.g., in southeastern California and British Columbia) could result in land use changes that reduce

the permeability of the landscape to native species (Batllori, Parisien, Parks, Moritz, & Miller, 2017). Similarly, the high climate connectivity value of the western slope of the Appalachians is potentially impacted by intensification of human land use. The high importance of the Arctic for climate connectivity may also be threatened by future expansion of the human footprint in that region.

Some approaches to climate adaptation planning avoid use of future climate projections due to the inherent uncertainty in forecasting future emissions and their effect on global climate (Beier, Hunter, & Anderson, 2015). However, we found that climate connectivity priorities were robust to uncertainty caused by variation in input data between alternative emission pathways (RCP 4.5 and 8.5) and AOGCMs. Priorities based on centrality derived from different AOGCMs showed less between-AOGCM variation than did the input climate data or climatic velocity metrics based on that climate data (Carroll et al., 2017). Conservation planners may place greater focus on sensitivity analyses of the effect of assumptions concerning dispersal behavior and analysis extent, rather than on parameter uncertainty arising from differing climate projections.

The high correlation between centrality results based on near-future and distant-future climate projections should offer planners more confidence that climate corridors protected based on shorter time horizons will remain valuable over longer time frames, assuming a linear trend in changes in climate. However, identification of continuous paths tracking climate over multiple intermediate time steps, as is possible using network flow approaches, would be a useful refinement of our approach that avoids such assumptions (Graham et al., 2010; Phillips et al., 2008).

## 4.2 | Relevance of graph-based models to planning for dispersal under climate change

Although highly simplified representations of dispersal, graph-based models are often more computationally feasible than more realistic dispersal simulations, allowing analyses at finer resolution or broader spatial extent (Adriaensen et al., 2003). While our approach is applicable at spatial extents ranging from continents to local regions, continental-extent analyses are an important initial step in discerning patterns that would not be evident in an analysis limited to a smaller extent, for example, an ecoregion (Rudnick et al., 2012). For example, because future climate analogs for some climate types will only occur outside an ecoregion, an analysis limited to the extent of a single ecoregion would not be able to evaluate connectivity for these climate types. Results from an analysis limited to the extent of a single ecoregion were only moderately correlated with values for the same region derived from the continental-extent analysis, suggesting that planners should compare metrics derived at broader and more limited extents to assess robustness of conclusions to spatial scale.

Because the two types of graph-based models (shortest-path and current-flow-based centrality) applied here make contrasting assumptions about the ability of dispersers to find optimal paths, comparison of their output provides complementary information about priority areas and helps assess robustness to assumptions about

dispersal behavior (Carroll et al., 2012; Carroll, Fredrickson, & Lacy, 2014; García Molinos et al., 2017). Shortest-path results can help identify a minimal “skeleton” of landscape linkages which may not be evident from current-flow results. Conversely, current-flow approaches identify both specific pinchpoints along this minimal network and broader regions with high importance for connectivity (Carroll et al., (2014); McRae et al., (2016)). Current flow results are also more biologically realistic in that they are more influenced by flow between nearby points than between distant pairs of points (Figure 1). However, the greater computational feasibility of shortest-path algorithms allows more detailed analyses comparing forward and backward climate connectivity areas, and results based on differing maximum dispersal distances. The relatively coarse resolution of our continental-extent analysis, however, limits our ability to identify fine-scale refugia important to species with limited dispersal capabilities (Stralberg et al., 2018).

The paths identified in our analysis are most relevant for terrestrial organisms that can migrate or establish stepping-stone populations at a rate similar to the climatic velocity projected for their climatic niche. If climatic velocity is high in relation to dispersal ability, assisted migration becomes the most relevant intervention, obviating the need to consider the intervening landscape (McLachlan, Hellmann, & Schwartz, 2007). Conversely, if dispersal ability is large in relation to climatic velocity, organisms may transit climatically hostile landscapes rapidly. Finally, if a species' dispersal rate is of a similar magnitude to the velocity of climate change, then both path-based velocity metrics (Dobrowski & Parks, 2016) and climate centrality become relevant in assessing conservation priorities.

However, several factors limit the comparability of the shortest-path lengths from our models with dispersal distances recorded from field observations. To the extent that published summaries of dispersal rates (Settele et al., 2015) are based on measurements of straight-line displacement, they may be more comparable to standard climatic velocity values than to circuitous climatic-resistance-based paths, which averaged 45% longer than straight-line displacements in our results (Supporting information Figure S8). Both climatic-resistance-based and straight-line velocity values are sensitive to how finely continuous climatic values are divided into types (Dobrowski & Parks, 2016; Hamann et al., 2015). The climate type width used here allow assessment of climatic tolerances narrower than those shown by most species, and can help inform conservation of locally-adapted populations, an often-ignored facet of the extinction crisis (Ceballos & Ehrlich, 2002). Graph-based assessments of climate connectivity derive their practical relevance not from direct comparability with field data on dispersal but because they provide a relative measure of climate exposure that is more realistic for many organisms than is straight-line climatic velocity, and allow planners to identify and protect landscape features of importance for broad-scale connectivity. Climate connectivity areas represent important conservation targets even in regions of high climatic velocity (red areas in Supporting information Figure S9) where unassisted migration will be feasible for a smaller subset of the biota.

### 4.3 | Coarse- and fine-filter approaches to assessing connectivity

Our approach resembles many previous studies in defining source and target areas based on climate data (i.e., climate analogs), effectively using climate types as a “coarse-filter” surrogate for biodiversity targets (Noss & Cooperrider, 1994). Alternatively, several studies have instead identified species-specific source and target areas using future species distributions based on climatic niche models. Schloss, Nunez, and Lawler (2012) used niche model projections to measure straight-line distance and velocity between current and future species climatic niches across the Western Hemisphere. Lawler, Ruesch, Olden, and McRae (2013) extended this niche-model-based approach by mapping current-flow-based paths between current and projected futures species niches. More recent work (Miller & McGill, 2018) has simulated dispersal of temperate tree species under climate change using detailed data on species-specific life histories.

Coarse- and fine-filter approaches are often seen as complementary (Tingley, Darling, & Wilcove, 2014), because coarse-filter analyses provide context by allowing a comprehensive depiction of patterns across climate space rather than being limited to the climatic niches of the subset of taxa for which distribution data are available (Brito-Morales et al., 2018). For example, coarse-filter analyses, especially at the resolution permitted by graph-based methods, allows identification and characterization of topographic features associated with climate connectivity areas in a manner that would be difficult using species-specific models.

### 4.4 | Future directions

Conservation planning under climate change forces us to consider novel questions regarding connectivity. For example, are the types of land use change that impede dispersal under climate change the same as those traditionally seen as fragmenting landscapes? What management strategies are relevant when climate connectivity areas are identified in agricultural or otherwise modified landscapes? Will climate connectivity paths for organisms which must avoid such human-modified landscapes exceed the dispersal ability of species of conservation concern? Our analysis, which does not incorporate anthropogenic factors into calculation of landscape resistance, can serve as context for future research which evaluates species-specific responses to anthropogenic and other nonclimatic habitat factors.

It would also be informative to develop similar graph-based analyses comparing current and paleoclimates to compare locations that potentially facilitated connectivity under past climate change with available data on past distribution shifts. It is likely that connectivity areas under future warming climates will differ from those under paleoclimates. However, some regions identified in our results such as the North Pacific Coast, Isthmus of Tehuantepec, and Appalachians may have also facilitated range shifts under past climate change due to their broad-scale topography and location in relation to the shape of the North American continent.

The robustness of our results to uncertainty from alternative AOGCMs and emissions pathways should give planners increased confidence in applying conservation priorities based on future climate projections. The sensitivity of results to model uncertainty should be expected given that the different approaches used here make contrasting assumptions concerning dispersal behavior. Planners should see these contrasting results as complementary information sources that must be viewed in context of the strengths and limitations of graph-based models. Although the metrics used here are necessarily simplified representations of real-world dispersal processes, they can add a missing dimension to climate adaptation planning by identifying landscape features which promote connectivity among refugia, a key management strategy under climate change (Heller & Zavaleta, 2009).

## ACKNOWLEDGMENTS

The authors dedicate this paper to the late Brad McRae, in appreciation of his contributions to advancing both this work and the broader field of connectivity conservation science. The manuscript benefited from suggestions by P. Elsen and two anonymous reviewers. Co-authors are listed in the order of relative contribution (SDC system). The Wilburforce Foundation provided support for the authors as part of the AdaptWest Climate Adaptation Planning Project (<https://adaptwest.databasin.org>; see site for data associated with this paper).

## ORCID

Carlos Carroll  <http://orcid.org/0000-0002-7697-8721>

Sean A. Parks  <https://orcid.org/0000-0002-2982-5255>

David R. Roberts  <http://orcid.org/0000-0002-3437-2422>

## REFERENCES

- Adriaensen, F., Chardon, J. P., De Blust, G., Swinnen, E., Villalba, S., Gulinck, H., & Matthysen, E. (2003). The application of “least-cost” modelling as a functional landscape model. *Landscape and Urban Planning*, *64*, 233–247. [https://doi.org/10.1016/S0169-2046\(02\)00242-6](https://doi.org/10.1016/S0169-2046(02)00242-6)
- Ahuja, R. K., Magnanti, T. L., & Orlin, J. B. (1993). *Network flows: Theory, algorithms, and applications*. Englewood Cliffs, NJ: Prentice Hall.
- Alagador, D., Cerdeira, J. O., & Araújo, M. B. (2016). Climate change, species range shifts and dispersal corridors: An evaluation of spatial conservation models. *Methods in Ecology and Evolution*, *7*, 853–866. <https://doi.org/10.1111/2041-210X.12524>
- Alagador, D., Cerdeira, J. O., Araújo, M. B., & Saura, S. (2014). Shifting protected areas: Scheduling spatial priorities under climate change. *Journal of Applied Ecology*, *51*, 703–713. <https://doi.org/10.1111/1365-2664.12230>
- Álvarez-Romero, J. G., Munguía-Vega, A., Beger, M., Mancha-Cisneros, M. M., Suárez-Castillo, A. N., Gurney, G. G., ... Torre, J. (2018). Designing connected marine reserves in the face of global warming. *Global Change Biology*, *24*, e671–e691. <https://doi.org/10.1111/gcb.13989>
- ASTER GDEM Validation Team (2009). *ASTER global DEM validation summary report*. METI & NASA, 28 pp. Retrieved from <https://asterweb.jpl.nasa.gov/gdem.asp>
- Battlori, E., Parisien, M. A., Parks, S. A., Moritz, M. A., & Miller, C. (2017). Potential relocation of climatic environments suggests high rates of climate displacement within the North American protection network. *Global Change Biology*, *23*, 3219–3230. <https://doi.org/10.1111/gcb.13663>
- Beier, P., Hunter, M. L., & Anderson, M. (2015). Special section: Conserving nature’s stage. *Conservation Biology*, *29*, 613–617.
- Brito-Morales, I., García Molinos, J., Schoeman, D. S., Burrows, M. T., Poloczanska, E. S., Brown, C. J., ... Richardson, A. J. (2018). Climate velocity can inform conservation in a Warming World. *Trends in Ecology and Evolution*, *33*, 441–457. <https://doi.org/10.1016/j.tree.2018.03.009>
- C.E.C. (1997). *Ecological regions of North America towards a common perspective*. Montréal, QC: Commission for Environmental Cooperation.
- C.E.C. (2010). *Terrestrial protected areas of North America, 2010*. Montréal, QC: Commission for Environmental Cooperation.
- Carroll, C., Fredrickson, R. J., & Lacy, R. C. (2014). Developing metapopulation connectivity criteria from genetic and habitat data to recover the endangered Mexican Wolf. *Conservation Biology*, *28*, 76–86. <https://doi.org/10.1111/cobi.12156>
- Carroll, C., Lawler, J. J., Roberts, D. R., & Hamann, A. (2015). Biotic and climatic velocity identify contrasting areas of vulnerability to climate change. *PLoS One*, *10*, e0140486. <https://doi.org/10.1371/journal.pone.0140486>
- Carroll, C., McRae, B. H., & Brookes, A. (2012). Use of linkage mapping and centrality analysis across habitat gradients to conserve connectivity of gray wolf populations in western North America. *Conservation Biology*, *26*, 78–87. <https://doi.org/10.1111/j.1523-1739.2011.01753.x>
- Carroll, C., Roberts, D. R., Michalak, J. L., Lawler, J. J., Nielsen, S. E., Stralberg, D., ... Wang, T. (2017). Scale-dependent complementarity of climatic velocity and environmental diversity for identifying priority areas for conservation under climate change. *Global Change Biology*, *23*, 4508–4520. <https://doi.org/10.1111/gcb.13679>
- Ceballos, G., & Ehrlich, P. R. (2002). Mammal population losses and the extinction crisis. *Science*, *296*, 904–907. <https://doi.org/10.1126/science.1069349>
- Daly, C., Halbleib, M., Smith, J. I., Gibson, W. P., Doggett, M. K., Taylor, G. H., ... Pasteris, P. P. (2008). Physiographically sensitive mapping of climatological temperature and precipitation across the conterminous United States. *International Journal of Climatology*, *28*, 2031–2064. <https://doi.org/10.1002/joc.1688>
- Dobrowski, S. Z., & Parks, S. A. (2016). Climate change velocity underestimates climate change exposure in mountainous regions. *Nature Communications*, *7*, 12349. <https://doi.org/10.1038/ncomms12349>
- Farr, T. G., Rosen, P. A., Caro, E., Crippen, R., Duren, R., Hensley, ... Alsdorf, D. (2007). The shuttle radar topography mission. *Reviews of Geophysics*, *45*, RG2004. <https://doi.org/10.1029/2005RG000183>
- García Molinos, J., Takao, S., Kumagai, N. H., Poloczanska, E. S., Burrows, M. T., Fujii, M., & Yamano, H. (2017). Improving the interpretability of climate landscape metrics: An ecological risk analysis of Japan’s Marine Protected Areas. *Global Change Biology*, *23*, 4440–4452. <https://doi.org/10.1111/gcb.13665>
- Graham, C. H., Vanderwal, J., Phillips, S. J., Moritz, C., & Williams, S. E. (2010). Dynamic refugia and species persistence: Tracking spatial shifts in habitat through time. *Ecography*, *33*, 1062–1069. <https://doi.org/10.1111/j.1600-0587.2010.06430.x>
- Hamann, A., Roberts, D. R., Barber, Q. E., Carroll, C., & Nielsen, S. E. (2015). Velocity of climate change algorithms for guiding conservation and management. *Global Change Biology*, *21*, 997–1004. <https://doi.org/10.1111/gcb.12736>
- Hastie, T., & Tibshirani, R. (1990). *Generalized additive models*, 1990. London, UK: Chapman and Hall.
- Heller, N. E., & Zavaleta, E. S. (2009). Biodiversity management in the face of climate change: A review of 22 years of recommendations.

- Biological Conservation*, 142, 14–32. <https://doi.org/10.1016/j.biocon.2008.10.006>
- Huang, J., Zhang, X., Zhang, Q., Lin, Y., Hao, M., Luo, Y., ... Zhang, J. (2017). Recently amplified arctic warming has contributed to a continual global warming trend. *Nature Climate Change*, 7, 875–879. <https://doi.org/10.1038/s41558-017-0009-5>
- Keppel, G., & Wardell-Johnson, G. W. (2012). Refugia: Keys to climate change management. *Global Change Biology*, 18, 2389–2391. <https://doi.org/10.1111/j.1365-2486.2012.02729.x>
- Knutti, R., Masson, D., & Gettelman, A. (2013). Climate model genealogy: Generation CMIP5 and how we got there. *Geophysical Research Letters*, 40, 1194–1199.
- Lawler, J. J., Ruesch, A. S., Olden, J. D., & McRae, B. H. (2013). Projected climate-driven faunal movement routes. *Ecology Letters*, 16, 1014–1022. <https://doi.org/10.1111/ele.12132>
- Littlefield, C. E., McRae, B. H., Michalak, J. L., Lawler, J. J., & Carroll, C. (2017). Connecting today's climates to future climate analogs to facilitate movement of species under climate change. *Conservation Biology*, 31, 1397–1408. <https://doi.org/10.1111/cobi.12938>
- Loarie, S. R., Duffy, P. B., Hamilton, H., Asner, G. P., Field, C. B., & Ackerly, D. D. (2009). The velocity of climate change. *Nature*, 462, 1052–1055. <https://doi.org/10.1038/nature08649>
- Mahony, C. R., Cannon, A. J., Wang, T., & Aitken, S. N. (2017). A closer look at novel climates: New methods and insights at continental to landscape scales. *Global Change Biology*, 23, 3934–3955. <https://doi.org/10.1111/gcb.13645>
- McGuire, J. L., Lawler, J. J., McRae, B. H., Nuñez, T. A., & Theobald, D. M. (2016). Achieving climate connectivity in a fragmented landscape. *Proceedings of the National Academy of Sciences*, 113, 7195–7200. <https://doi.org/10.1073/pnas.1602817113>
- McLachlan, J. S., Hellmann, J. J., & Schwartz, M. W. (2007). A framework for debate of assisted migration in an era of climate change. *Conservation Biology*, 21, 297–302. <https://doi.org/10.1111/j.1523-1739.2007.00676.x>
- McRae, B. H., & Beier, P. (2007). Circuit theory predicts gene flow in plant and animal populations. *Proceedings of the National Academy of Sciences*, 104, 19885–19890. <https://doi.org/10.1073/pnas.0706568104>
- McRae, B. H., Popper, K., Jones, A., Schindel, M., Buttrick, S., Hall, K., ... Platt, J. (2016). *Conserving nature's stage: Mapping omnidirectional connectivity for resilient terrestrial landscapes in the Pacific Northwest*. Portland, OR: The Nature Conservancy. Retrieved from <https://nature.org/resilience/NW>.
- Miller, K. M., & McGill, B. J. (2018). Land use and life history limit migration capacity of eastern tree species. *Global Ecology and Biogeography*, 27, 57–67. <https://doi.org/10.1111/geb.12671>
- Mora, C., Frazier, A. G., Longman, R. J., Dacks, R. S., Walton, M. M., Tong, E. J., ... Giambelluca, T. W. (2013). The projected timing of climate departure from recent variability. *Nature*, 502, 183–187. <https://doi.org/10.1038/nature12540>
- Newman, M. (2010). *Networks: An introduction*. Oxford, UK: Oxford University Press.
- Noss, R. F., & Cooperrider, A. (1994). *Saving nature's legacy: Protecting and restoring biodiversity*. Covelo, CA: Island Press.
- Nunez, T. A., Lawler, J. J., McRae, B. H., Pierce, D. J., Krosby, M. B., Kavanagh, D. M., ... Tewksbury, J. J. (2013). Connectivity planning to address climate change. *Conservation Biology*, 27, 407–416. <https://doi.org/10.1111/cobi.12014>
- Ordóñez, A., & Williams, J. W. (2013). Climatic and biotic velocities for woody taxa distributions over the last 16,000 years in eastern North America. *Ecology Letters*, 16, 773–781.
- Phillips, S. J., Williams, P., Midgley, G., & Archer, A. (2008). Optimizing dispersal corridors for the Cape Proteaceae using network flow. *Ecological Applications*, 18, 1200–1211. <https://doi.org/10.1890/07-0507.1>
- Rao, C. R. (1982). Diversity and dissimilarity coefficients: A unified approach. *Theoretical Population Biology*, 21, 24–43. [https://doi.org/10.1016/0040-5809\(82\)90004-1](https://doi.org/10.1016/0040-5809(82)90004-1)
- Rudnick, D. A., Ryan, S. J., Beier, P., Cushman, S. A., Dieffenbach, F., Epps, C. W., ... Trombulak, S. C. (2012). The role of landscape connectivity in planning and implementing conservation and restoration priorities. *Issues in Ecology*, 16, 1–20.
- Schloss, C. A., Nunez, T. A., & Lawler, J. J. (2012). Dispersal will limit ability of mammals to track climate change in the Western Hemisphere. *Proceedings of the National Academy of Sciences*, 109, 8606–8611. <https://doi.org/10.1073/pnas.1116791109>
- Settle, J., Scholes, R., Betts, R. A., Bunn, S., Leadley, P., & Nepstad, D., ... Moreno, J. M. (2015). Terrestrial and inland water systems. In Intergovernmental Panel on Climate Change (Ed.), *Climate change 2014 impacts, adaptation and vulnerability: Part A: Global and sectoral aspects* (pp. 271–360). Cambridge, UK: Cambridge University Press.
- Stralberg, D., Carroll, C., Pedlar, J. H., Wiley, C. B., McKenney, D. W., & Nielsen, S. E. (2018). Macrorefugia for North American trees and songbirds: Climatic limiting factors and multi-scale topographic influences. *Global Ecology and Biogeography*, 27, 690–703. <https://doi.org/10.1111/geb.12731>
- Tingley, M. W., Darling, E. S., & Wilcove, D. S. (2014). Fine- and coarse-filter conservation strategies in a time of climate change. *Annals of the New York Academy of Sciences*, 1322, 92–109.
- Van Etten, J., & Hijmans, R. J. (2010). A geospatial modelling approach integrating archaeobotany and genetics to trace the origin and dispersal of domesticated plants. *PLoS One*, 5, e12060. <https://doi.org/10.1371/journal.pone.0012060>
- Venter, O., Sanderson, E. W., Magrath, A., Allan, J. R., Beher, J., Jones, K. R., ... Watson, J. E. M. (2016). Global terrestrial Human Footprint maps for 1993 and 2009. *Scientific Data*, 3, 160067. <https://doi.org/10.1038/sdata.2016.67>
- Wang, T., Hamann, A., Spittlehouse, D., & Carroll, C. (2016). Locally downscaled and spatially customizable climate data for historical and future periods for North America. *PLoS One*, 11, e0156720. <https://doi.org/10.1371/journal.pone.0156720>
- Wilson, M. F. J., O'Connell, B., Brown, C., Guinan, J. C., Grehan, A. J. (2007). Multiscale terrain analysis of multibeam bathymetry data for habitat mapping on the continental slope. *Marine Geodesy*, 30, 3–35. <https://doi.org/10.1080/01490410701295962>

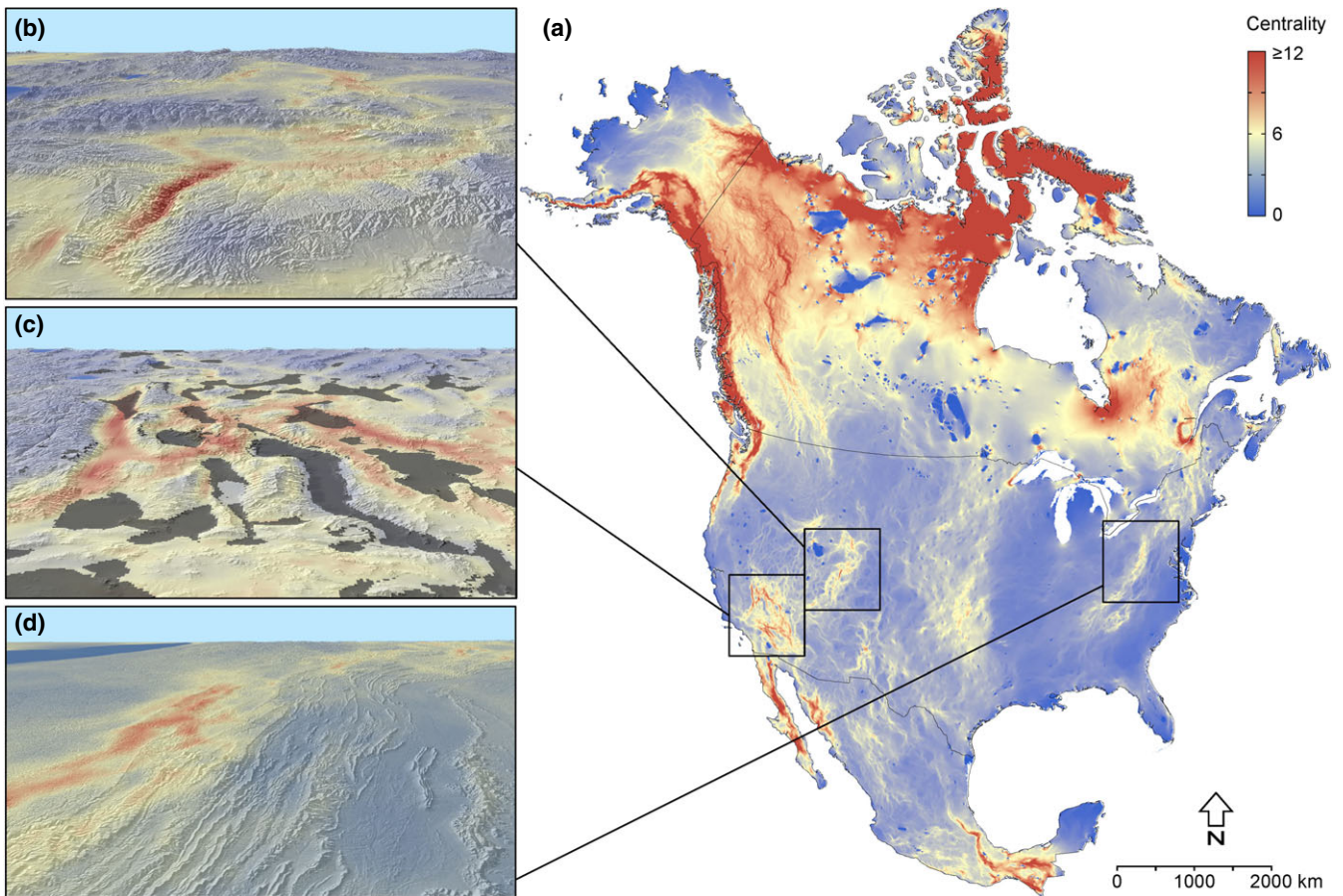
## SUPPORTING INFORMATION

Additional supporting information may be found online in the Supporting Information section at the end of the article.

**How to cite this article:** Carroll C, Parks SA, Dobrowski SZ, Roberts DR, . Climatic, topographic, and anthropogenic factors determine connectivity between current and future climate analogs in North America. *Glob Change Biol*. 2018;00:1–14. <https://doi.org/10.1111/gcb.14373>

# Graphical Abstract

The contents of this page will be used as part of the graphical abstract of html only.  
It will not be published as part of main article.



The persistence of many species under climate change will depend on our ability to identify and protect areas that facilitate dispersal to newly climatically suitable habitat. We used centrality metrics to identify climate connectivity areas across North America by delineating paths between current climate types and their future analogs that avoided non-analogous climates. Paths were funneled along north-south trending passes and valley systems and away from areas of novel and disappearing climates. Climate connectivity areas, where many potential dispersal paths overlap, are distinct from refugia and thus poorly captured by many existing conservation strategies.